Superbunching pseudothermal light

Yu Zhou and Fu-li Li
MOE Key Laboratory for Nonequilibrium Synthesis and Modulation of Condensed Matter, Department of Applied Physics, Xi'an Jiaotong University, Xi'an 710049, China

Bin Bai, Hui Chen, Jianbin Liu,* and Zhuo Xu
Electronic Materials Research Laboratory, Key Laboratory of the Ministry of Education & International Center for Dielectric Research, Xi'an Jiaotong University, Xi'an 710049, China

Huaibin Zheng
MOE Key Laboratory for Nonequilibrium Synthesis and Modulation of Condensed Matter, Department of Applied Physics, Xi'an Jiaotong University, Xi'an 710049, China
and Electronic Materials Research Laboratory, Key Laboratory of the Ministry of Education & International Center for Dielectric Research, Xi'an Jiaotong University, Xi'an 710049, China
(Received 16 February 2017; published 3 May 2017)

A simple superbunching pseudothermal light source is introduced based on common instruments such as laser, lenses, pinholes, and ground glasses. $g^{(2)}(0) = 3.66 \pm 0.02$ is observed in the suggested scheme by employing two rotating ground glasses. Quantum and classical theories are employed to interpret the observed superbunching effect. It is predicted that $g^{(2)}(0)$ can reach 2^N if N rotating ground glasses were employed. These results are helpful to understand the physics of superbunching. The proposed superbunching pseudothermal light may serve as a type of light to study the second- and higher-order coherence of light and have potential application in improving the visibility of thermal light ghost imaging.

DOI: 10.1103/PhysRevA.95.053809

I. INTRODUCTION

Two-photon bunching was first observed by Hanbury Brown and Twiss in 1956 [1,2], in which randomly emitted photons by thermal light source have the tendency to come in bunches rather than randomly. Much attention was drawn to this bunching effect shortly after it was reported. Some researchers repeated Hanbury Brown and Twiss's experiments and got negative results [3,4]. It was later understood that the negative results were due to the response time of the detection system being much longer than the coherence time of the measured light [5]. Classical theory was first employed to interpret the bunching effect [6–9]. Then quantum theory was also employed to interpret the same effect [10–13]. It is now well accepted that the two-photon bunching effect of thermal light can be explained by both quantum and classical theories [12–14]. The full quantum explanation of the bunching effect given by Glauber greatly deepens our understanding of optical coherence. The Hanbury Brown and Twiss experiments [1,2] and Glauber's quantum optical coherence theory [12,13] are usually regarded as the cornerstones of modern quantum optics [15].

The experimental setup employed by Hanbury Brown and Twiss [1,2], which is known as the Hanbury Brown–Twiss (HBT) interferometer, plays an important role in measuring the second-order coherence of light and photon statistics in quantum optics [5,16]. The second-order coherence of light can be described by the normalized second-order coherence function introduced by Glauber [12,13]. For a light beam in a HBT interferometer, two-photon bunching is defined as $g^{(2)}(0) > g^{(2)}(\tau)$ $(\tau \neq 0)$, where $g^{(2)}(\tau)$ is the normalized second-order coherence function and τ is the time difference between two photon detection events within a two-photon coincidence count. On the contrary, antibunching is defined as $g^{(2)}(0) < g^{(2)}(\tau)$ $(\tau \neq 0)$, which is usually regarded as a nonclassical effect [5]. It is well known that $g^{(2)}(0)$ equals 2 for thermal light [1,2,5]. For the bunched light, the phrase two-photon *superbunching* is usually employed if $g^{(2)}(0)$ is larger than 2 [17].

Two-photon superbunching is usually introduced by nonlinear interaction between light and atoms [18–26], quantum dots [27–29], or nonlinear medium [30–35], etc. The efficiency of generating two-photon superbunching effect with nonlinear interaction is usually very low and high precision alignment is always required in adjusting the experimental setup [18–35]. It is tempting to generate two-photon superbunching effect with linear effect. Hong *et al.* observed $g^{(2)}(0) = 2.4 \pm 0.1$ in a linear system via multiple two-photon path interference [36]. They further predicted that higher value of $g^{(2)}(0)$ could be reached by adding more paths. However, it is a big experimental challenge if more paths are added in their scheme [36]. In this paper, we will introduce a different and much simpler scheme for superbunching with classical light in a linear system, which is called superbunching pseudothermal light. The corresponding quantum and classical interpretations of the superbunching effect in our scheme are of great importance to understand the physics of superbunching. The proposed superbunching pseudothermal light source may find possible applications in the second- and higher-order interference of light [5,16] and high-visibility ghost imaging with classical light [37].

The paper is organized as follows. In Sec. II, we will introduce the superbunching pseudothermal light source

*liujianbin@xjtu.edu.cn

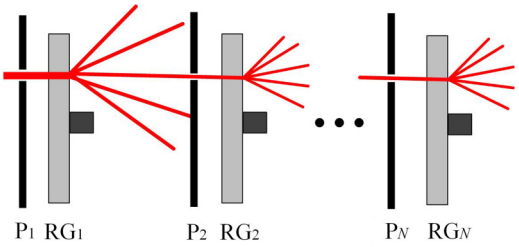

FIG. 1. Superbunching pseudothermal light source. P_j: the jth pinhole. RG_j: the jth rotating ground glass. The pinhole before RG_j is employed to filter out the light beam within one coherence area of pseudothermal light generated by RG_{j-1} ($j = 2,3,\ldots,N$).

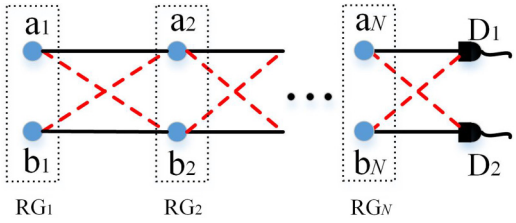

FIG. 2. Different paths for two photons to trigger a two-photon coincidence count in superbunching scheme. a_j and b_j are the possible positions of photons on RG_j ($j = 1,2,\ldots,N$). D_1 and D_2 are two single-photon detectors in a HBT interferometer. The outputs of these two detectors are sent to a two-photon coincidence count detection system to measure the two-photon coincidence count, which is not shown in the figure.

and employ two-photon interference theory to calculate the second-order coherence function. The experimental setup with two rotating ground glasses is employed to observe two-photon superbunching effect in Sec. III. The discussions about the physics of superbunching and an alternative scheme for superbunching pseudothermal light source are in Sec. IV. Section V summarizes our conclusions.

II. THEORY

A. Superbunching pseudothermal light with N rotating ground glasses

The proposed superbunching pseudothermal light source is shown in Fig. 1, where P_j and RG_j are the jth pinhole and rotating ground glass, respectively ($j = 1,2,\ldots,N$). A coherent light beam is incident to RG_1 after passing through P_1. The scattered light is then filtered out by P_2. The filtered light beam is within the same transverse coherence area of pseudothermal light generated by RG_1. The incident light before RG_2 is coherent and there will be interference pattern after RG_2. Another pinhole and RG can be put after RG_2 in the same manner and the process can be repeated for N (positive integer) RGs.

If a single-mode continuous-wave laser light beam is employed as the input before P_1 in Fig. 1, the scattered light after RG_1 is pseudothermal light [38], which has been applied extensively in thermal light ghost imaging [39–42], the second- and higher-order interference of thermal light [43–46]. The photons in light beam after N ($N \geqslant 2$) RGs will be superbunched, which means the normalized second-order coherence function, $g^{(2)}(0)$, will exceed 2.

The HBT interferometer [1,2] is employed in the scheme shown in Fig. 1 to measure the second-order coherence function. When there is only one RG in the scheme, there are two different alternatives for two photons in pseudothermal light to trigger a two-photon coincidence count. One is that photon a (short for photon at position a) is detected by D_1 (short for detector 1) and photon b is detected by D_2. The other one is that photon a is detected by D_2 and photon b is detected by D_1. If these two different alternatives are indistinguishable, the second-order coherence function is [10,11,37,47,48]

$$G_1^{(2)}(\mathbf{r}_1,t_1;\mathbf{r}_2,t_2) = \langle |A_1 + A_2|^2 \rangle, \tag{1}$$

where $(\mathbf{r}_j,t_j)$ is the space-time coordinates for the photon detection event at D_j ($j = 1$ and 2). $\langle \cdots \rangle$ is the ensemble average by taking all the possible realizations into account. A_1 and A_2 are the corresponding probability amplitudes for the above two alternatives, respectively. Based on the calculations in [37] and Appendix A of this paper, the value of $g^{(2)}(0)$ can be approximately estimated by the ratio between the number of total terms and the number of autocorrelation terms in Eq. (1). There are four terms after the modulus square is calculated and two autocorrelation terms. The normalized second-order coherence function, $g^{(2)}(0)$, equals 2 in this case, which is consistent with the conclusions in [8–11].

When there are two RGs, there are four different alternatives for two photons to trigger a two-photon coincidence count in the scheme in Fig. 1. These four alternatives are a_1-a_2-D_1 and b_1-b_2-D_2, a_1-a_2-D_2 and b_1-b_2-D_1, a_1-b_2-D_2 and b_1-a_2-D_1, and a_1-b_2-D_1 and b_1-a_2-D_2, respectively. a_1-a_2-D_1 means photon at a_1 goes to a_2 and then is detected by D_1. The meanings of other symbols are similar. If these four different alternatives are indistinguishable, the second-order coherence function with two RGs is [47,48]

$$G_2^{(2)}(\mathbf{r}_1,t_1;\mathbf{r}_2,t_2) = \langle |A_1 + A_2 + A_3 + A_4|^2 \rangle, \tag{2}$$

where A_1, A_2, A_3, and A_4 are the corresponding probability amplitudes for the above four alternatives, respectively. The number of total terms after modulus square in Eq. (2) is 4^2. The number of autocorrelation terms is 4. Hence $g^{(2)}(0)$ equals $4^2/4$ for two RGs in Fig. 1, in which superbunching is expected.

The same method can be employed to calculate the normalized second-order coherence function of N RGs in Fig. 1. There are 2^N different alternatives for two photons to trigger a two-photon coincidence count for N RGs in Fig. 1, which can be understood in the following way. There are 2^1 and 2^2 different alternatives for one and two RGs in Fig. 1, respectively. We can assume that there are 2^{N-1} different alternatives to trigger a two-photon coincidence count for $N-1$ RGs in Fig. 1. By adding the Nth RG, there will be two more possible positions, a_N and b_N, for the photons as shown in Fig. 2. There are 2^{N-1} different alternatives, for the photon at a_N is detected by D_1 and the photon at b_N is detected by D_2. When exchanging the orders, i.e., the photon at a_N is detected by D_2 and the photon at b_N is detected by D_1, there are 2^{N-1} different alternatives, too. Hence the total number of alternatives to trigger a two-photon coincidence count for N RGs in Fig. 1 is $2^{N-1} + 2^{N-1}$, which equals 2^N.

If all the 2^N different alternatives are indistinguishable, the second-order coherence function for N RGs is

$$G_N^{(2)}(\mathbf{r}_1,t_1;\mathbf{r}_2,t_2) = \left\langle \left| \sum_{j=1}^{2^N} A_j \right|^2 \right\rangle, \tag{3}$$

where A_j is the jth probability amplitude for two photons at a_1 and b_1 are detected by D_1 and D_2 to trigger a two-photon coincidence count. The number of total terms in Eq. (3) after modulus square is $(2^N)^2$ and the number of autocorrelation terms is 2^N. The normalized second-order coherence function of N RGs in the scheme shown in Fig. 1 is

$$g_N^{(2)}(0) = \frac{(2^N)^2}{2^N} = 2^N, \tag{4}$$

where two-photon superbunching is expected for N ($N \geqslant 2$) RGs.

B. Second-order temporal coherence function of superbunching pseudothermal light

In this section, we will calculate the second-order temporal coherence functions for one and two RGs in the superbunching pseudothermal light scheme, respectively.

The Feynman photon propagator for a point light source is [49]

$$K_{\alpha\beta} = \frac{\exp[-i(\omega_\alpha t_{\alpha\beta} - \mathbf{k}_{\alpha\beta}\cdot\mathbf{r}_{\alpha\beta})]}{r_{\alpha\beta}}, \tag{5}$$

which is the same as the Green function for a point light source in classical optics [50]. $\mathbf{r}_{\alpha\beta}$ equals $\mathbf{r}_\beta - \mathbf{r}_\alpha$, which is the position vector of the photon at $\mathbf{r}_\alpha$ that goes to $\mathbf{r}_\beta$. $\mathbf{r}_\alpha$ and $\mathbf{r}_\beta$ are two position vectors. $r_{\alpha\beta}$ is the distance between $\mathbf{r}_\alpha$ and $\mathbf{r}_\beta$, which equals $|\mathbf{r}_{\alpha\beta}|$. $\mathbf{k}_{\alpha\beta}$ and ω_α are the wave vector and frequency of the photon at $\mathbf{r}_\alpha$ that goes to $\mathbf{r}_\beta$, respectively. $t_{\alpha\beta}$ equals $t_\beta - t_\alpha$, which is the time for the photon at $\mathbf{r}_\alpha$ that goes to $\mathbf{r}_\beta$. t_α and t_β are the time for the photon at $\mathbf{r}_\alpha$ and $\mathbf{r}_\beta$, respectively.

For simplicity, we will concentrate on the temporal correlation. The propagator in Eq. (5) can be simplified as

$$K_{\alpha\beta} \propto e^{-i\omega_\alpha(t_\beta - t_\alpha)} \tag{6}$$

by ignoring the spatial part. The second-order coherence function in Eq. (1) can be written as

$$G_1^{(2)}(t_1,t_2) = \langle |e^{i\varphi_{a1}} K_{a1D1} e^{i\varphi_{b1}} K_{b1D2} + e^{i\varphi_{a1}} K_{a1D2} e^{i\varphi_{b1}} K_{b1D1}|^2 \rangle, \tag{7}$$

where φ_{a1} and φ_{b1} are the initial phases of photons at a_1 and b_1, respectively. The initial phases of photons in thermal light are random [51]. t_1 and t_2 are short for t_{D1} and t_{D2}, which are the time for photon detection events at D_1 and D_2, respectively. Substituting Eq. (6) into Eq. (7), it is straightforward to have

$$G_1^{(2)}(t_1 - t_2) \propto 2 + 2\,\mathrm{Re}[e^{-i\omega_{a1}(t_1-t_2)} e^{-i\omega_{b1}(t_1-t_2)}], \tag{8}$$

where Re is the real part of the complex expression. Assuming the frequency bandwidth of the light scattered by RG_1 is $\Delta\omega_1$, the normalized second-order temporal coherence function for one RG in the scheme shown in Fig. 1 is [37,52]

$$g_1^{(2)}(t_1 - t_2) = 1 + \mathrm{sinc}^2 \frac{\Delta\omega_1(t_1 - t_2)}{2}, \tag{9}$$

where $\mathrm{sinc}(x)$ equals $\sin(x)/x$. When the value of $|t_1 - t_2|$ is large enough, $g_1^{(2)}(t_1 - t_2)$ equals 1, which means the detections of these two photons are independent in this condition. $g_1^{(2)}(t_1 - t_2)$ equals 2 when $t_1 - t_2$ equals zero, which means photons in thermal light have tendency to come in bunches. This phenomenon is the two-photon bunching effect, which was first observed by Hanbury Brown and Twiss [1,2].

With the same method above, we can have the second-order temporal coherence function for two RGs in the scheme shown in Fig. 1,

$$g_2^{(2)}(t_1 - t_2) = \left[1 + \mathrm{sinc}^2 \frac{\Delta\omega_1(t_1 - t_2)}{2}\right] \times \left[1 + \mathrm{sinc}^2 \frac{\Delta\omega_2(t_1 - t_2)}{2}\right], \tag{10}$$

where the detail calculations can be found in Appendix A. $\Delta\omega_1$ and $\Delta\omega_2$ are the frequency bandwidths of pseudothermal light at RG_1 and RG_2, respectively. When the value of $|t_1 - t_2|$ is large enough, $g_2^{(2)}(t_1 - t_2)$ equals 1, which means two photon detection events are independent. When $t_1 - t_2$ equals zero, $g_2^{(2)}(t_1 - t_2)$ equals 4, which means two-photon superbunching can be observed.

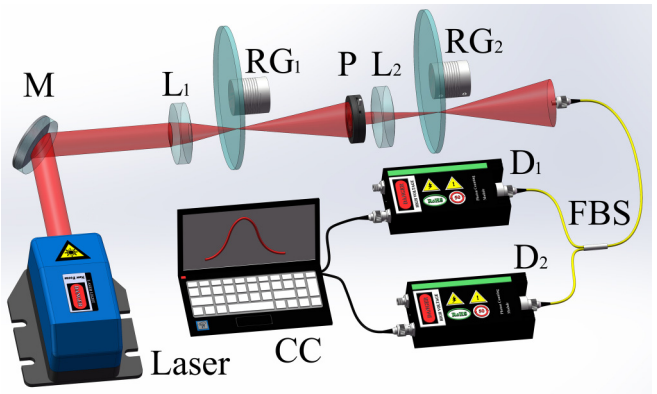

FIG. 3. Experimental setup for superbunching pseudothermal light source with two RGs. Laser: single-mode continuous-wave laser. M: mirror. L: lens. RG: rotating ground glass. P: pinhole. FBS: nonpolarized 50:50 fiber beam splitter. D: single-photon detector. CC: two-photon coincidence count detection system.

III. EXPERIMENTS

The experimental setup to observe superbunching pseudothermal light with two RGs is shown in Fig. 3. The employed laser is a linearly polarized single-mode continuous-wave laser with central wavelength at 780 nm and frequency bandwidth of 200 kHz (Newport, SWL-7513). M is a mirror. L_1 is a focus lens with focus length of 50 mm. RG_1 and RG_2 are two rotating ground glasses. P is a pinhole. The distance between L_1 and RG_1 is 50 mm. The distance between RG_1 and the pinhole is 240 mm. The transverse coherence length of pseudothermal light generated by RG_1 is 4 mm in the pinhole plane. The

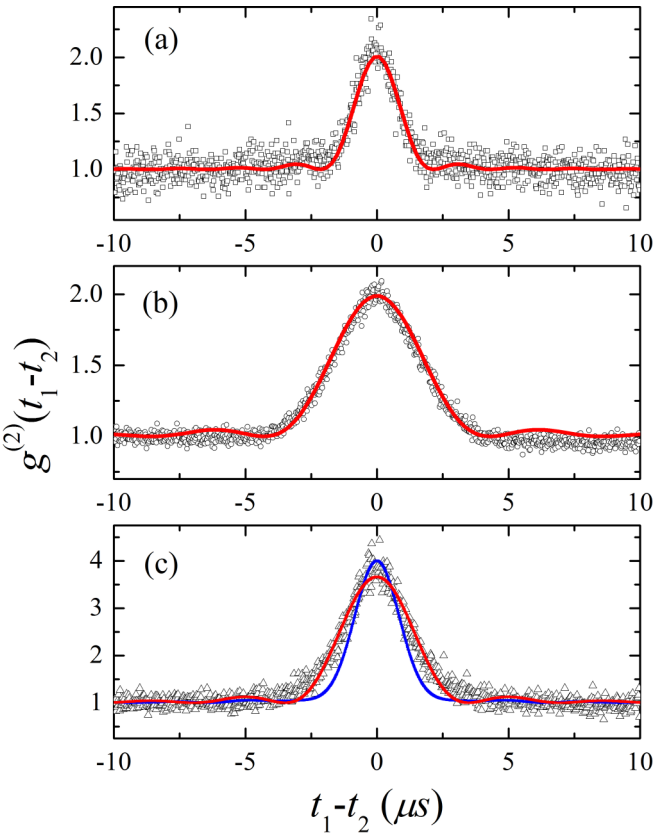

FIG. 4. Measured second-order temporal coherence functions. $g^{(2)}(t_1 - t_2)$ is the normalized second-order coherence function. $t_1 - t_2$ is the time difference between two single-photon detection events within a two-photon coincidence count. The squares, circles, and triangles are measured results. The red lines are theoretical fittings by employing Eq. (9). Panel (a) is measured when RG_1 is not rotating while RG_2 is rotating at 12 Hz. Panel (b) is measured when RG_1 is rotating at 40 Hz while RG_2 is not rotating. Panel (c) is measured when RG_1 and RG_2 are rotating at 40 and 12 Hz, respectively. The blue line in (c) is the product of the red lines in (a) and (b).

diameter of the pinhole is 1.2 mm, which is less than the coherence length. Only the light within one coherence area can pass the pinhole. The second lens with focus length of 25 mm, L_2, is employed to focus the light onto RG_2. The distance between L_2 and RG_2 is 28 mm, which is determined by minimizing the size of light spot on RG_2. The reason why the distance between L_2 and RG_2 is larger than the focus length of L_2 is that the light scattered by RG_1 is diffuse instead of parallel. A nonpolarized 50:50 fiber beam splitter (FBS) is employed to measure the second-order temporal coherence function. The distance between RG_2 and the collector of FBS is 700 mm. The diameter of the collector of FBS is 5 μm, which is much less than the coherence length of pseudothermal light generated by RG_2 in the same plane ($\sim$13 mm). D_1 and D_2 are two single-photon detectors (PerkinElmer, SPCM-AQRH-14-FC). CC is a two-photon coincidence count detection system (Becker & Hickl GmbH, DPC-230).

We first measure the second-order temporal coherence function of usual pseudothermal light [38]. Figure 4(a) shows the measured normalized second-order temporal coherence function when RG_1 is not rotating while RG_2 is rotating at 12 Hz. $g^{(2)}(t_1 - t_2)$ is the normalized second-order coherence function and $t_1 - t_2$ is the time difference between the two single-photon detection events within a two-photon coincidence count. The squares are the measured results, which are normalized according to the background. The red line is theoretical fitting by employing Eq. (9). The measured coherence time and $g^{(2)}(0)$ of pseudothermal light in Fig. 4(a) are 1.08 ± 0.01 μs and 2.01 ± 0.02, respectively. Figure 4(b) shows the measured results when RG_1 is rotating at 40 Hz while RG_2 is not rotating. The circles are measured results and the red line is the fitting of the measured data by employing Eq. (9). The measured coherence time and $g^{(2)}(0)$ of pseudothermal light in Fig. 4(b) are 2.15 ± 0.03 μs and 1.99 ± 0.01, respectively. Figure 4(c) is the measured second-order coherence function when RG_1 and RG_2 are rotating with speeds of 40 and 12 Hz, respectively. The triangles are measured results and the red line is theoretical fitting of the data by employing Eq. (9). The measured coherence time in Fig. 4(c) is 1.74 ± 0.02 μs. The ratio between the peak and the background in Fig. 4(c) is much larger than the ones in Figs. 4(a) and 4(b). The normalized second-order coherence function, $g^{(2)}(0)$, equals 3.66 ± 0.02, in which two-photon superbunching is observed.

The blue line in Fig. 4(c) is the product of the two fitted lines in Figs. 4(a) and 4(b). It is consistent with the measured results except the calculated line is narrower. The reason may be the conditions to measure Fig. 4(c) are not exactly the same as the ones to measure Fig. 4(a). When measuring the temporal coherence function in Fig. 4(a), we manually rotate RG_1 to a certain position to ensure that the single-photon counting rates of both detectors are at 5000 c/s level. The size of the light spot on RG_2 did not vary during the measurement. However, RG_1 is rotating during the measurement of coherence function in Fig. 4(c), in which the size of the light spot on RG_2 varies during the measurement. The difference between these two measurements may cause the deviation between the blue line and the measured results in Fig. 4(c). However, two-photon superbunching effect is observed in Fig. 4(c) from either the red line or the blue line, which means that the principle of superbunching pseudothermal light source in Fig. 1 works.

IV. DISCUSSIONS

A. Why two-photon superbunching can be observed in our scheme

In the last two sections, we have employed two-photon interference theory to predict that two-photon superbunching can be observed in the scheme shown in Fig. 1 and experimentally confirmed it. The key to observed superbunching in our scheme is that all the different alternatives to trigger a two-photon coincidence count are in principle indistinguishable when there is more than one RG. If these different alternatives to trigger a two-photon coincidence count are distinguishable, the second-order coherence function is [48]

$$G_N^{(2)}(\mathbf{r}_1,t_1;\mathbf{r}_2,t_2) = \left\langle \sum_{j=1}^{2^N} |A_j|^2 \right\rangle, \tag{11}$$

where the probabilities, instead of probability amplitudes, are summed. There are no cross terms in Eq. (11). The ratio between the number of total terms and the number of autocorrelation terms is 1, which means $g_N^{(2)}(0)$ equals 1. No two-photon superbunching can be observed if all the alternatives are distinguishable.

In the scheme shown in Fig. 1, the necessary and sufficient condition for these different alternatives indistinguishable is that the photons are indistinguishable [53]. Photons are indistinguishable if they are within the same coherence volume [5,38]. Coherence volume equals the product of transverse coherence area and longitudinal coherence length. If a pinhole with diameter less than the transverse coherence length of light is employed to filter the light, the photons passing through the pinhole are within the same coherence area. All the photons within the coherence time are indistinguishable in this case. This is what we have done in the scheme in Fig. 1 and in the experiment in Fig. 3. A pinhole between RG_j and RG_{j+1} is employed to filter the photons within one coherence area of pseudothermal light generated by RG_j ($j = 1,2,\ldots,N$). All the different alternatives are indistinguishable if a pinhole is employed to filter the photons within the same coherence area after every RG.

In the early work by Hong *et al.* [36], two-photon superbunching is also observed by adding more alternatives via a modified Michelson interferometer. They experimentally observed $g^{(2)}(0)$ equals 2.4 ± 0.1 and theoretically proved that $g^{(2)}(0)$ will increase to 2×1.5^N if N modified Michelson interferometers were inserted into their scheme. However, it is very difficult to insert more than one modified Michelson interferometer into their scheme since special requirements should be satisfied for the two mirrors in the Michelson interferometer [36]. More two-photon paths are added through inserting more modified Michelson interferometers into their scheme [36]. In our scheme, more two-photon paths are added through adding more rotating ground glasses and pinholes. We have observed $g^{(2)}(0) = 3.66 \pm 0.02$ by employing two RGs and one pinhole. Furthermore, the value of $g^{(2)}(0)$ can be increased to 2^N if N RGs were employed in our scheme. Comparing to the scheme by Hong *et al.* [36], our superbunching pseudothermal light source is much simpler and the value of $g^{(2)}(0)$ increases faster when more alternatives were added in the scheme. Another difference between these two schemes is that two-photon superbunching is observed in spatial domain in [36] and temporal domain in our research.

B. Revised scheme and classical interpretation

The superbunching pseudothermal light source in Fig. 1 can also be understood in classical theory [12–14]. The intensity of light after one RG obeys negative exponential distribution [54],

$$P(I) = \frac{1}{\langle I \rangle} \exp\left(-\frac{I}{\langle I \rangle}\right), \tag{12}$$

where $\langle I \rangle$ is the average intensity of the scattered light. If a pinhole is employed to filter the light within one coherence area, the intensity of light after the pinhole will obey Eq. (12) when the ground glass is rotating. Even though the intensity of the filtered light is not constant, it is coherent since it is within one coherence area [38]. This light beam can be incident to another RG to generate pseudothermal light. Based on the results in Appendix B, the second-order moments of the light intensity after n ($n = 2$, 3, 4, and 5) RGs is

$$\langle I^2 \rangle = \langle I \rangle^2 2^n. \tag{13}$$

The normalized second-order coherence function is [5]

$$g_n^{(2)}(0) \equiv \frac{\langle I^2 \rangle}{\langle I \rangle^2} = 2^n. \tag{14}$$

We did not prove this equation for any value of n. However, it is confirmed that this equation is true for n equals 2, 3, 4, and 5. The result in Eq. (14) is consistent with the one in Eq. (4).

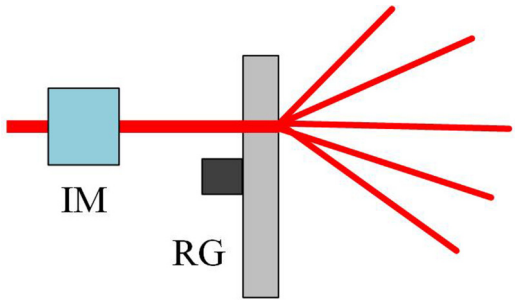

FIG. 5. Revised superbunching pseudothermal light scheme. The intensity modulator (IM) before rotating ground glass (RG) is used to modulate the intensity of the incident light without randomizing the phase.

Most energy of the incident light in the scheme shown in Fig. 1 is wasted due to scattering. From the classical point of view, all the RGs before the last one are employed to introduce certain intensity distribution. An intensity modulator (IM) can be employed to modulate the light intensity to obey the same distribution as the one of multiple RGs. Two-photon superbunching can also be observed in the scheme shown in Fig. 5 if suitable intensity modulation is applied by IM.

There are no multiple alternatives before RG to trigger a two-photon coincidence count in the scheme shown in Fig. 5. How to understand the superbunching effect can also be observed in the scheme shown in Fig. 5 as the one in Fig. 1. For simplicity, let us take two RGs, for example, to explain the physics of these two schemes. In the scheme shown in Fig. 1, the incident light before RG_2 is filtered by a pinhole from the pseudothermal light generated by RG_1. The intensity before RG_2 obeys negative exponential distribution [54]. This phenomenon can be understood by two-photon interference since there are different and indistinguishable alternatives to trigger a two-photon coincidence count. However, from a classical point of view, the filtered light before RG_2 in Fig. 1 can be mimicked by a light beam with the same negative exponential distribution as the one scattered by RG_1. There is no difference for RG_2 whether the incident light is filtered by a pinhole in pseudothermal light or directly modulated by an IM as long as the intensities of light beams obey the same distribution and the light is coherent. The discussions can be generalized to the N RGs case.

V. CONCLUSIONS

In summary, we have proposed a superbunching pseudothermal light source based on simple laboratory instruments such as laser, lenses, rotating ground glasses, and pinholes, etc. Two-photon interference theory is employed to interpret the two-photon superbunching effect and it is found that the key to observe superbunching in our scheme is that all the different alternatives to trigger a two-photon coincidence count are in principle indistinguishable. $g^{(2)}(0) = 3.66 \pm 0.02$ is observed with two RGs in the superbunching scheme and it is predicted that $g^{(2)}(0)$ can reach 2^N if N RGs were employed. Based on the conclusions in classical theory, we suggested a different but equivalent superbunching pseudothermal light scheme by replacing all the RGs before the last one with an intensity modulator. The revised scheme can be employed to observe superbunching as long as the intensity of the modulated light obeys certain distribution. Light intensity obeying negative exponential distribution and related distributions is discussed in this paper. It is interesting to study whether superbunching can be observed or not when the intensity obeys other types of distributions.

The observed two-photon superbunching is in the temporal domain, which is helpful to improve the visibility of temporal ghost imaging with classical light [55]. Whether the spatial superbunching can be realized by analogy of the temporal superbunching is an interesting topic, too. The discussions of superbunching, in both the quantum and classical theories, are helpful to understand the physics of two-photon superbunching. We believe that the simple superbunching pseudothermal light source will be an important tool to study thermal light ghost imaging, the second- and higher-order interference of thermal light, and other possible applications of thermal light.

ACKNOWLEDGMENTS

This project is supported by National Natural Science Foundation of China (Grant No. 11404255), Doctoral Fund of Ministry of Education of China (Grant No. 20130201120013), the 111 Project of China (Grant No. B14040), and the Fundamental Research Funds for the Central Universities.

APPENDIX A: SECOND-ORDER TEMPORAL COHERENCE FUNCTION OF TWO RGs

There are four different alternatives for two photons to trigger a two-photon coincidence count when two RGs are in the scheme shown in Fig. 1. The first one is a_1-a_2-D_1 and b_1-b_2-D_2, which means the photon at a_1 goes to a_2 and then is detected by D_1 and the photon at b_1 goes to b_2 and then is detected by D_2. The other three alternatives are a_1-a_2-D_2 and b_1-b_2-D_1, a_1-b_2-D_2 and b_1-a_2-D_1, and a_1-b_2-D_1 and b_1-a_2-D_2, respectively. If these four different alternatives are indistinguishable, the second-order coherence function of two RGs in the scheme shown in Fig. 1 is

$$\begin{aligned} &G_2^{(2)}(\mathbf{r}_1,t_1;\mathbf{r}_2,t_2) \\ &\quad = \langle |A_{a1a2D1}A_{b1b2D2} + A_{a1a2D2}A_{b1b2D1} \\ &\qquad + A_{a1b2D2}A_{b1a2D1} + A_{a1b2D1}A_{b1a2D2}|^2 \rangle. \end{aligned} \tag{A1}$$

With the same method as the one for one RG, we only consider the temporal part. There will be 16 terms after modulus square is evaluated in Eq. (A1). The four autocorrelation terms only contribute to the background. There are 12 cross-correlation terms left, which can be categorized into three groups. We can have the result of one group by calculating one term from the same group.

The first term that needs to be calculated is $A_{a1a2D1}A_{b1b2D2}A^*_{a1a2D2}A^*_{b1b2D1}$, where A^*_{a1a2D2} is the complex conjugate of A_{a1a2D2}. The probability amplitude of two successive and independent events equals the product of these two different probability amplitudes [48]. A_{a1a2D1} can be written as $A_{a1a2}A_{a2D1}$. Other terms can be simplified in the same way. Substituting this relation and Eq. (6) into the term above, we have

$$\begin{aligned} &A_{a1a2D1}A_{b1b2D2}A^*_{a1a2D2}A^*_{b1b2D1} \\ &\quad = e^{-i\omega_{a1}(t_{a2}-t_{a1})}e^{-i\omega_{a2}(t_1-t_{a2})}e^{-i\omega_{b1}(t_{b2}-t_{b1})}e^{-i\omega_{b2}(t_2-t_{b2})} \\ &\qquad \times e^{i\omega_{a1}(t_{a2}-t_{a1})}e^{i\omega_{a2}(t_2-t_{a2})}e^{i\omega_{b1}(t_{b2}-t_{b1})}e^{i\omega_{b2}(t_1-t_{b2})} \\ &\quad = e^{-i\omega_{a2}(t_1-t_2)}e^{i\omega_{b2}(t_1-t_2)}. \end{aligned} \tag{A2}$$

The last term on the right-hand side of Eq. (A2) is similar to the last term of Eq. (8). If the frequency bandwidth of thermal light scattered by RG_2 is $\Delta\omega_2$, $A_{a1a2D1}A_{b1b2D2}A^*_{a1a2D2}A^*_{b1b2D1}$ can be calculated as

$$\begin{aligned} &A_{a1a2D1}A_{b1b2D2}A^*_{a1a2D2}A^*_{b1b2D1} \\ &\quad = \int\int_{\omega_0-\frac{\Delta\omega_2}{2}}^{\omega_0+\frac{\Delta\omega_2}{2}} e^{-i\omega_{a2}(t_1-t_2)}e^{i\omega_{b2}(t_1-t_2)}d\omega_{a2}d\omega_{b2} \\ &\quad = (\Delta\omega_2)^2\mathrm{sinc}^2\frac{\Delta\omega_2(t_1-t_2)}{2}. \end{aligned} \tag{A3}$$

ω_0 is the central frequency of light and $\mathrm{sinc}(x)$ equals $\sin(x)/x$. The other three terms, $A^*_{a1a2D1}A^*_{b1b2D2}A_{a1a2D2}A_{b1b2D1}$, $A_{a1b2D1}A_{b1a2D2}A^*_{a1b2D2}A^*_{b1a2D1}$, and $A^*_{a1b2D1}A^*_{b1a2D2}A_{a1b2D2}A_{b1a2D1}$, in the same group have the same result as the one of Eq. (A3).

The second term that needs to be calculated is $A_{a1a2D1}A_{b1b2D2}A^*_{a1b2D2}A^*_{b1a2D1}$. With the same method above, we have

$$\begin{aligned} &A_{a1a2D1}A_{b1b2D2}A^*_{a1b2D2}A^*_{b1a2D1} \\ &\quad = e^{-i\omega_{a1}(t_{a2}-t_{a1})}e^{-i\omega_{a2}(t_1-t_{a2})}e^{-i\omega_{b1}(t_{b2}-t_{b1})}e^{-i\omega_{b2}(t_2-t_{b2})} \\ &\qquad \times e^{i\omega_{a1}(t_{b2}-t_{a1})}e^{i\omega_{b2}(t_2-t_{b2})}e^{i\omega_{b1}(t_{a2}-t_{b1})}e^{i\omega_{a2}(t_1-t_{a2})} \\ &\quad = e^{-i\omega_{a1}(t_{a2}-t_{b2})}e^{i\omega_{b1}(t_{a2}-t_{b2})}. \end{aligned} \tag{A4}$$

Assuming the frequency bandwidth of thermal light scattered by RG_1 is $\Delta\omega_1$, $A_{a1a2D1}A_{b1b2D2}A^*_{a1b2D2}A^*_{b1a2D1}$ can be calculated as

$$\begin{aligned} &A_{a1a2D1}A_{b1b2D2}A^*_{a1b2D2}A^*_{b1a2D1} \\ &\quad = \int\int_{\omega_0-\frac{\Delta\omega_1}{2}}^{\omega_0+\frac{\Delta\omega_1}{2}} e^{-i\omega_{a1}(t_{a2}-t_{b2})}e^{i\omega_{b1}(t_{a2}-t_{b2})}d\omega_{a1}d\omega_{b1} \\ &\quad = (\Delta\omega_1)^2\mathrm{sinc}^2\frac{\Delta\omega_1(t_{a2}-t_{b2})}{2}, \end{aligned} \tag{A5}$$

where the central frequency is assumed to be the same during scattering in different RGs. t_{a2} is related to t_1 by the relation

$t_{a2} = t_1 - r_{a2D1}/c$, where r_{a2D1} is the distance between $\mathbf{r}_{a2}$ and $\mathbf{r}_{D1}$. c is the velocity of light in the vacuum. In a similar way, t_{b2} is related to t_2 by $t_{b2} = t_2 - r_{b2D2}/c$. Point light source and symmetrical positions for D_1 and D_2 are assumed in the calculations of temporal correlation. r_{a2D1} equals r_{b2D2}. $t_{a2} - t_{b2}$ can be replaced by $t_1 - t_2$ in Eq. (A5),

$$A_{a1a2D1}A_{b1b2D2}A^*_{a1b2D2}A^*_{b1a2D1} = (\Delta\omega_1)^2\mathrm{sinc}^2\frac{\Delta\omega_1(t_1-t_2)}{2}. \tag{A6}$$

The terms, $A^*_{a1a2D1}A^*_{b1b2D2}A_{a1b2D2}A_{b1a2D1}$, $A_{a1a2D2}A_{b1b2D1}A^*_{a1b2D1}A^*_{b1a2D2}$, and $A^*_{a1a2D2}A^*_{b1b2D1}A_{a1b2D1}A_{b1a2D2}$, in the same group have the same result as the one in Eq. (A6).

The third term that needs to be calculated is $A_{a1a2D1}A_{b1b2D2}A^*_{a1b2D1}A^*_{b1a2D2}$, which is

$$\begin{aligned}&A_{a1a2D1}A_{b1b2D2}A^*_{a1b2D1}A^*_{b1a2D2}\\ &= e^{-i\omega_{a1}(t_{a2}-t_{a1})}e^{-i\omega_{a2}(t_1-t_{a2})}e^{-i\omega_{b1}(t_{b2}-t_{b1})}e^{-i\omega_{b2}(t_2-t_{b2})}\\ &\quad\times e^{i\omega_{a1}(t_{b2}-t_{a1})}e^{i\omega_{b2}(t_1-t_{b2})}e^{i\omega_{b1}(t_{a2}-t_{b1})}e^{i\omega_{a2}(t_2-t_{a2})}\\ &= e^{-i\omega_{a1}(t_{a2}-t_{b2})}e^{i\omega_{b1}(t_{a2}-t_{b2})}e^{-i\omega_{a2}(t_1-t_2)}e^{i\omega_{b2}(t_1-t_2)}.\end{aligned} \tag{A7}$$

Integrating over the frequency bandwidths of thermal light scattered by RG_1 and RG_2, we have

$$\begin{aligned}&A_{a1a2D1}A_{b1b2D2}A^*_{a1b2D1}A^*_{b1a2D2}\\ &= (\Delta\omega_1\Delta\omega_2)^2\mathrm{sinc}^2\frac{\Delta\omega_1(t_1-t_2)}{2}\mathrm{sinc}^2\frac{\Delta\omega_2(t_1-t_2)}{2}.\end{aligned} \tag{A8}$$

The other three terms, $A^*_{a1a2D1}A^*_{b1b2D2}A_{a1b2D1}A_{b1a2D2}$, $A_{a1a2D2}A_{b1b2D1}A^*_{a1b2D2}A^*_{b1a2D1}$, and $A^*_{a1a2D2}A^*_{b1b2D1}A_{a1b2D2}A_{b1a2D1}$, in the same group have the same result as the one in Eq. (A8).

In the calculations of Eqs. (A3) and (A5), we have ignored the integral of the constant, 1, for RG_1 and RG_2, respectively. If we take this factor into account and also integrate the autocorrelation terms, the second-order temporal coherence function with two RGs in the scheme in Fig. 1 is

$$\begin{aligned}G^{(2)}_2(t_1-t_2) \propto 4(\Delta\omega_1\Delta\omega_2)^2\Bigg[&1+\mathrm{sinc}^2\frac{\Delta\omega_1(t_1-t_2)}{2}\\ &+\mathrm{sinc}^2\frac{\Delta\omega_2(t_1-t_2)}{2}\rangle+\mathrm{sinc}^2\frac{\Delta\omega_1(t_1-t_2)}{2}\\ &\times\mathrm{sinc}^2\frac{\Delta\omega_2(t_1-t_2)}{2}\Bigg].\end{aligned} \tag{A9}$$

All the 16 terms in Eq. (A1) are calculated. Rearranging the terms on the right-hand side of Eq. (A9), the normalized second-order temporal coherence function can be expressed as

$$\begin{aligned}g^{(2)}_2(t_1-t_2) = &\left[1+\mathrm{sinc}^2\frac{\Delta\omega_1(t_1-t_2)}{2}\right]\\ &\times\left[1+\mathrm{sinc}^2\frac{\Delta\omega_2(t_1-t_2)}{2}\right],\end{aligned} \tag{A10}$$

in which Eq. (10) is obtained.

APPENDIX B: CALCULATIONS OF $g^2(0)$ IN CLASSICAL THEORY

We will follow the method given by Goodman to show how the second-order coherence function in the scheme shown in Fig. 1 can be calculated in classical theory [54]. The probability density function of pseudothermal light generated by scattering single-mode continuous-wave laser light on a rotating ground glass is negative exponential distribution [38]. If the intensity of the incident light varies, the conditional density function of the scattered light should be

$$P_{I|x}(I|x) = \frac{1}{x}\exp\left(-\frac{I}{x}\right), \tag{B1}$$

where x is proportional to the intensity of the incident light. If the incident light is filtered out as the one shown in Fig. 1, the intensity, x, obeys negative exponential distribution, too. The density distribution of the light intensity after RG_2 is

$$P_I(I) = \int_0^\infty \frac{1}{x}\exp\left(-\frac{I}{x}\right)\frac{1}{\langle I\rangle}\exp\left(-\frac{x}{\langle I\rangle}\right)dx, \tag{B2}$$

where $\langle I\rangle$ is the average intensity of the scattered light after RG_2. Equation (B2) can be simplified as [54]

$$P_I(I) = \frac{2}{\langle I\rangle}K_0\left(2\sqrt{\frac{I}{\langle I\rangle}}\right), \tag{B3}$$

where $K_0(x)$ is the modified Bessel function of the second kind, order zero. The qth moment of the intensity is

$$\langle I^q\rangle = \int_0^\infty I^q P_I(I)dI = \langle I\rangle^q(q!)^2. \tag{B4}$$

In classical theory, the normalized second-order coherence function is defined as [5]

$$g^{(2)}(\mathbf{r}_1,t_1;\mathbf{r}_2,t_2) = \frac{\langle I(\mathbf{r}_1,t_1)I(\mathbf{r}_2,t_2)\rangle}{\langle I(\mathbf{r}_1,t_1)\rangle\langle I(\mathbf{r}_2,t_2)\rangle}, \tag{B5}$$

where $I(\mathbf{r}_j,t_j)$ is the intensity of light at space-time coordinate $(\mathbf{r}_j,t_j)$ ($j = 1$ and 2). When these two detectors are at symmetrical positions, the normalized second-order coherence function can be simplified as

$$g^{(2)}(0) = \frac{\langle I^2\rangle}{\langle I\rangle^2}. \tag{B6}$$

Substituting Eq. (B4) into Eq. (B6), the normalized second-order coherence function with two RGs in Fig. 1 equals 4, which is consistent with the result of Eq. (4) in quantum theory.

With the same method, we can calculate the normalized second-order coherence function for more than two RGs. If there are three RGs, the input intensity of RG_3 is given by Eq. (B3); the density function of the light intensity after RG_3 is given by

$$P_I(I) = \int_0^\infty \frac{2}{x}K_0\left(2\sqrt{\frac{I}{x}}\right)\frac{1}{\langle I\rangle}\exp\left(-\frac{x}{\langle I\rangle}\right)dx. \tag{B7}$$

There is no analytical expression for Eq. (B7). However, only the moment is needed to calculate the normalized

second-order coherence function. With the help of Eqs. (B4) and (B7), the qth moment of the light intensity after three RGs is

$$\langle I^q \rangle = \langle I \rangle^q (q!)^3. \tag{B8}$$

The corresponding normalized second-order coherence function, $g^{(2)}(0)$, equals 8. With the same method above, the qth moments of intensity after four and five RGs are $\langle I \rangle^q (q!)^4$ and $\langle I \rangle^q (q!)^5$, respectively, which correspond to the normalized second-order coherence functions equal to 16 and 32, respectively. These results are consistent with the one in Eq. (4).

Employing classical theory to calculate the normalized second-order coherence function for more than five RGs is straightforward. However, the process may be cumbersome. The results above are sufficient to prove that if we can employ an intensity modulator (IM) to modulate the intensity of light to obey negative exponential distribution before RG, $g^{(2)}(0)$ should equal 4. For the condition of more than two RGs, numerical method can be employed to calculate the intensity distribution and then apply the distribution on the IM. The experimental realization of superbunching pseudothermal light with $g^{(2)}(0) = 2^N$ should be possible for N larger than 2 in the scheme shown in Fig. 5.

[1] R. H. Brown and R. Q. Twiss, Nature (London) **177**, 27 (1956).
[2] R. H. Brown and R. Q. Twiss, Nature (London) **178**, 1046 (1956).
[3] E. Brannen and H. I. S. Ferguson, Nature (London) **178**, 481 (1956).
[4] H. I. S. Ferguson, Nature (London) **179**, 956 (1957).
[5] L. Mandel and E. Wolf, *Optical Coherence and Quantum Optics* (Cambridge University Press, New York, 1995), p. 714.
[6] A. T. Forrester, R. A. Gudmundsen, and P. O. Johnson, Phys. Rev. **99**, 1691 (1955).
[7] A. T. Forrester, Am. J. Phys. **24**, 192 (1956).
[8] R. Hanbury Brown and R. Q. Twiss, Proc. R. Soc. London Ser. A **242**, 300 (1957).
[9] R. Hanbury Brown and R. Q. Twiss, Proc. R. Soc. London Ser. A **243**, 291 (1958).
[10] E. M. Purcell, Nature (London) **178**, 1449 (1956).
[11] U. Fano, Am. J. Phys. **29**, 539 (1961).
[12] R. J. Glauber, Phys. Rev. **130**, 2529 (1963).
[13] R. J. Glauber, Phys. Rev. **131**, 2766 (1963).
[14] E. C. G. Sudarshan, Phys. Rev. Lett. **10**, 277 (1963).
[15] R. J. Glauber, Rev. Mod. Phys. **78**, 1267 (2006).
[16] M. O. Scully and M. S. Zubairy, *Quantum Optics* (Cambridge University Press, Cambridge, UK, 1997).
[17] Z. Ficek and S. Swain, *Quantum Interference and Coherence: Theory and Experiments* (Springer Science+Business Media, Inc., New York, 2005).
[18] M. Lipeles, R. Novick, and N. Tolk, Phys. Rev. Lett. **15**, 690 (1965).
[19] R. D. Kaul, J. Opt. Soc. Am. **56**, 1262 (1966).
[20] C. A. Kocher and E. D. Commins, Phys. Rev. Lett. **18**, 575 (1967).
[21] S. A. Akhmanov, D. P. Krindach, A. P. Sukhorukov, and R. V. Khokhlov, JETP Lett. **6**, 38 (1967).
[22] S. Swain, P. Zhou, and Z. Ficek, Phys. Rev. A **61**, 043410 (2000).
[23] A. Auffèves, D. Gerace, S. Portolan, A. Drezet, and M. F. Santos, New J. Phys. **13**, 093020 (2011).
[24] I. C. Hoi, T. Palomaki, J. Lindkvist, G. Johansson, P. Delsing, and C. M. Wilson, Phys. Rev. Lett. **108**, 263601 (2012).
[25] T. Grujic, S. R. Clark, D. Jaksch, and D. G. Angelakis, Phys. Rev. A **87**, 053846 (2013).
[26] D. Bhatti, J. von Zanthier, and G. S. Agarwal, Sci. Rep. **5**, 17335 (2016).
[27] F. Albert, C. Hopfmann, S. Reitzenstein, C. Schneider, S. Höfling, L. Worschech, M. Kamp, W. Kinzel, A. Forchel, and I. Kanter, Nat. Commun. **2**, 366 (2011).
[28] F. Jahnke, C. Gies, M. Aßmann, M. Bayer, H. A. M. Leymann, A. Foerster, J. Wiersig, C. Schneider, M. Kamp, and S. Höfling, Nat. Commun. **7**, 11540 (2016).
[29] C. Redlich, B. Lingnau, S. Holzinger, E. Schlottmann, S. Kreinberg, C. Schneider, M. Kamp, S. Höfling, J. Wolters, S. Reitzenstein, and K. Lüdge, New J. Phys. **18**, 063011 (2016).
[30] D. N. Klyshko, A. N. Penin, and B. F. Polkovniko, JETP Lett. **11**, 5 (1970).
[31] D. C. Burnham and D. L. Weinberg, Phys. Rev. Lett. **25**, 84 (1970).
[32] C. O. Alley and Y. H. Shih, in *Proceedings of the 2nd International Symposium on Foundations of Quantum Mechanics*, edited by M. Namuki *et al.* (Phys. Soc. Japan, Tokyo, 1987); Phys. Rev. Lett. **61**, 2921 (1988).
[33] Z. Y. Ou and L. Mandel, Phys. Rev. Lett. **61**, 50 (1988).
[34] T. Sh. Iskhakov, A. M. Pérez, K. Yu. Spasibko, M. V. Chekhova, and G. Leuchs, Opt. Lett. **37**, 1919 (2012).
[35] Y. Bromberg, Y. Lahini, E. Small, and Y. Silberberg, Nat. Photon. **4**, 721 (2010).
[36] P. L. Hong, J. B. Liu, and G. Q. Zhang, Phys. Rev. A **86**, 013807 (2012).
[37] Y. H. Shih, *An Introduction to Quantum Optics* (Taylor and Francis Group, LLC, FL, London, 2011).
[38] W. Martienssen and E. Spiller, Am. J. Phys. **32**, 919 (1964).
[39] A. Gatti, E. Brambilla, M. Bache, and L. A. Lugiato, Phys. Rev. Lett. **93**, 093602 (2004).
[40] J. Cheng and S. S. Han, Phys. Rev. Lett. **92**, 093903 (2004).
[41] A. Valencia, G. Scarcelli, M. D'Angelo, and Y. H. Shih, Phys. Rev. Lett. **94**, 063601 (2005).
[42] Y. Cai and S. Y. Zhu, Phys. Rev. E **71**, 056607 (2005).
[43] L. Mandel, Phys. Rev. A **28**, 929 (1983).
[44] J. B. Liu and Y. H. Shih, Phys. Rev. A **79**, 023819 (2009).
[45] J. B. Liu, Y. Zhou, W. T. Wang, R. F. Liu, K. He, F. L. Li, and Z. Xu, Opt. Express **21**, 19209 (2013).
[46] J. B. Liu, Y. Zhou, F. L. Li, and Z. Xu, Europhys. Lett. **105**, 64007 (2014).
[47] R. P. Feynman, *QED: The Strange Theory of Light and Matter* (Princeton University, Princeton, NJ, 1985).
[48] R. P. Feynman and A. R. Hibbs, *Quantum Mechanics and Path Integrals* (McGraw-Hill, Inc., New York, 1965).
[49] M. E. Peskin and D. V. Schroeder, *An Introduction to Quantum Field Theory* (Westview Press, Boulder, 1995).

[50] M. Born and E. Wolf, *Principles of Optics*, 7th ed. (Cambridge University Press, Cambridge, UK, 1999).

[51] R. Loudon, *The Quantum Theory of Light*, 3rd ed. (Oxford University Press, New York, 2000).

[52] Y. Zhou, J. Simon, J. B. Liu, and Y. H. Shih, Phys. Rev. A **81**, 043831 (2010).

[53] J. B. Liu, Y. Zhou, H. B. Zheng, H. Chen, F-L. Li, and Z. Xu, Opt. Commun. **354**, 79 (2015).

[54] J. W. Goodman, *Speckle Phenomena in Optics: Theory and Applications* (Ben Roberts & Company, Greenwood Village, 2007).

[55] P. Ryczkowski, M. Barbier, A. T. Friberg, J. M. Dudley, and G. Genty, Nat. Photon. **10**, 167 (2016).